Obtaining and Main Dielectric Properties of Ba0.6Pb0.4TiO3/graphene Oxide Composite

Ryszard Skulski (ryszard.skulski@us.edu.pl)
Support Services for Interactive Learning https://orcid.org/0000-0003-2192-4045
Dariusz Bochenek
Uniwersytet Slaski w Katowicach
Dagmara Brzezińska
University of Silesia
Leszek Stobinski
Politechnika Warszawska
Przemysław Niemiec
Uniwersytet Slaski w Katowicach
Grzegorz Dercz
Uniwersytet Slaski w Katowicach
Katarzyna Osińska
Uniwersytet Slaski w Katowicach

Research Article

Keywords: composite, ferroelectrics, graphene oxide, microstructure, dielectric properties, hysteresis loop

Posted Date: June 16th, 2020

DOI: https://doi.org/10.21203/rs.3.rs-35095/v1

Version of Record: A version of this preprint was published at Journal of Materials Science: Materials in Electronics on April 11th, 2021. See the published version at https://doi.org/10.1007/s10854-021-05792-y.

Abstract

In this paper there is described the technology of obtaining and results of investigations of microstructure, XRD, SEM, main dielectric properties, electrical conductivity measurements and *P-E* hysteresis loops of $Ba_{0.6}Pb_{0.4}TiO_3$/graphene oxide composite (abbr. BPT/GO). In the final step of technology, the samples have been sintered using the Spark Plasma Sintering (SPS) method. Diffraction patterns of BPT/GO composite exhibit lines which can be related with perovskite structure, as well as reveal additional lines that can be derived from the initial component oxides. Investigations of electrical conductivity suggest that the PTCR effect occurs at temperatures up to about 120°C. Dielectric hysteresis loops below 90°C are wide and typical for materials with rather high electrical conductivity. The hysteresis loop obtained at 120°C is more typical for ferroelectrics. The obtained material is interesting, however it is probably possible to find better conditions of obtaining it and/or a better composition.

1. Introduction

Barium titanate ($BaTiO_3$ - abbr. BT) is one of the most known ferroelectric materials with perovskite structure. Because of its excellent dielectric, piezoelectric and ferroelectric properties it can be used as for example in piezoelectric sensors, multi-layer ceramic capacitors (MLCC), ferroelectric random access memories (FRAM), optoelectronic devices, actuators, and similar. Ferroelectric properties of barium titanate can be modified by introducing a wide variety of substitutions or dopants into their main structure [1] or even by the addition of second phases to form composites materials [2], which leads to large changes in the mechanical and dielectric properties.

For some applications Curie temperature of BT is too low, so solid solutions based on BT are used for example $Ba_{1-x}Pb_xTiO_3$. One of first works concerning $Ba_{1-x}Pb_xTiO_3$ was work [3]. In solid solution $Ba_{1-x}Pb_xTiO_3$ the Curie temperature linearly decreases from about 500 °C for $x = 1$ to about 120 °C for $x = 0$. More recent data on $Ba_{0.6}Pb_{0.4}TiO_3$ ceramics doped by special glass are presented, for instance, in work [4].

According to work [5] the graphene (G) is a single atomic plane of graphite, which – and this is essential – is sufficiently isolated from its environment to be considered free-standing. Atomic planes are of course familiar to everyone as constituents of bulk crystals but one-atom-thick materials such as graphene remained unknown. Graphene is the thinnest known material in the universe and the strongest ever measured.

In the recent years, in the literature we can find certain papers describing the results of the addition of flake Graphene (G) and flake Graphene Oxide (GO) into various materials, allowing to obtain new composite materials. It generally it provides the new possibilities of changing and improving physicochemical properties. For example the introduction of graphene blocks decreases the final grain size. For this reason, the conductivity of the barium titanate-graphene composites does not monotonically increase with carbon content. In [6] the composites of $BaTiO_3$/graphene with different

concentrations of the conductive graphene phase have been investigated. In work [6] $BaTiO_3$/graphene powders (between 0.1 and 0.6%) have been prepared from $BaTiO_3$ powders which were dispersed in distilled water and then mixed with graphene oxide, ball milled and finally sintered using Spark Plasma Sintering (SPS) in vacuum. Finally, it has been shown in [6] that the addition of the graphene pins the growth of grains of the ceramic matrix, leading to a change of the microstructure at low filler concentrations. As a consequence, the composites exhibit two percolation thresholds and their dielectric properties are not only determined by the dielectric properties of the constituents and their relative fractions, but also by the microstructure of the composite. Finally, grain sizes decrease with the increasing content of graphene.

In work [7], $BaTiO_3$/graphene composites were prepared with the wt.% of graphene up to 4%. The temperature dependence and the absolute values of resistivity and the Seebeck coefficient indicate that below 2%, the composites behave as n-type semiconductors, whereas over that GO content there is a change towards a more metallic electrical conduction regime. Concluding, the authors of [7] stated that ceramic/graphene composites are promising to tailor the thermo power and develop a new thermoelectric material for applications well above room temperature.

Another example of composite material with G and GO we can find in work [8]. Material obtained in [8] has been prepared for hybrid devices for multi-valued memory system. There are also many another examples of composite materials. As an examples we can give ceramic composites ferroelectric/ferrite [9–11].

In this paper, we describe the ferroelectric-graphene composite in which ferroelectric component is the solid solution of $Ba_{0.6}Pb_{0.4}TiO_3$ (BPT). We describe the technology of obtaining and main physical properties of $Ba_{0.6}Pb_{0.4}TiO_3$/graphene oxide (BPT/GO) composite with 1.6 wt.% of graphene oxide flakes. The samples were prepared using a simple processing route starting from $Ba_{0.6}Pb_{0.4}TiO_3$ (BPT) powders and an aqueous dispersion of graphene oxide, followed by Spark Plasma Sintering.

2. Material And Methods

The technology of obtaining of the BPT/GO composite employed by us was the following. We used commercial powders $BaTiO_3$ (Aldrich, purity: 99.9%, grains < 5 μm) and $PbTiO_3$ (Aldrich, purity: 99%, grains < 2 μm). The powders have been weighted and mixed at room temperature, in the proportion of 6/4 (what was supposed to provide the chemical composition $Ba_{0.6}Pb_{0.4}TiO_3$), and then were subsequently milled and mixed together with an agate mortar for 2 h. Melting of the oxides was carried out at 900 °C. In the next step, 1.6 wt.% of Graphene Oxide (GO) obtained in the way described in [12] (Faculty of Chemical and Process Engineering, Warsaw University of Technology, Warsaw) has been added. According to the thermogravimetric analysis [12], at the temperature of 200 °C, graphene oxide GO is almost fully thermally reduced to the form of rGO (reduced Graphene Oxide), decreasing the amount of oxygen groups from approx. 50 wt.% in GO to a few wt.% in rGO. The still remaining oxygen groups, covalently linked to the structure of rGO, are OH and C = O. In the final step, the samples have been sintered using the Spark

Plasma Sintering (SPS) method (The Institute of Advancing Manufacturing Technology, Cracow, Poland). The simple and frequently used method of sintering of ceramics is so called conventional sintering or free sintering (FS). The main problem during using this method is low relative density. Spark plasma sintering (SPS) (and hot pressing sintering HP) led produce fine ceramics with high density. The dependency of sample temperature as a function of time in SPS process used by us is presented in Fig. 1. The time of holding the sample at the temperature of about 1000 °C is very important since at this temperature during long time rGO is already fully reduced to pure carbon (graphite - GR) [12, 13].

Microstructure and EDS (Energy Dispersive Spectrometry) tests were carried out using a Field Emission Scanning Electron Microscope (Jeol Ltd., JEOL JSM–7100 TTL LV, Tokyo, Japan). Prior to the SEM/EDS analyses, the samples were coated with gold to provide electrical conductivity and avoid any charging effects.

X-ray measurements for obtained composite samples were performed using a (PANalytical, Phillips X'Pert Pro, Eindhoven, The Netherlands) diffractometer ($Cu–K_{\alpha}$ radiation). The data were collected at room temperature in the 2θ range from 10 to 80°, in the steps of 0.02 degrees, with the integration time of 4 s/step.

The dielectric measurements were performed using an LCR meter (QuadTech, Inc., 1920 Precision LCR meter, Maynard, MA, USA) during a heating cycle (in temperature range from 20 °C to 450 °C), at frequencies of the measurement field from 0.1 kHz to 1.0 MHz.

D.c. electrical conductivity has been measured using an electrometer (Keithley Instruments, Inc., 6517B, Cleveland, OH, USA) within the temperature range from 20 °C to 450 °C. *P-E* ferroelectric hysteresis loops were investigated using a Sawyer–Tower circuit and a high voltage amplifier (Matsusada Precision Inc., HEOPS–5B6, Kusatsu, Japan), in the temperature range from room temperature to 130 °C. The data were stored on a computer disc using an A/D, D/A transducer card (National Instruments) and LabView computer program.

3. Results

The measured apparent density of the BPT/GO composite after the SPS process was 6.07 g/cm^3. For the assumed composition adopting theoretical densities: 6.02 g/cm^3 for $BaTiO_3$, 7.52 g/cm^3 for $PbTiO_3$ and 2.09 g/cm^3 for hexagonal graphite GR, the theoretical density of our sample should be 6.55 g/cm^3. Therefore, the apparent density measured experimentally is equal to about 93% of the calculated theoretical density.

The analysis of SEM images for the BPT/GO composite with 1.6 wt.% GO for three magnifications is shown in Fig. 2 and Fig. 3 (after etching the surface).

It is seen that the grains generally do not have optimal shapes. The grains are heavily fused together, and their breakthrough occurs mainly by seed. However, during cracking, the grains do not disintegrate into

small fragments i.e. their surface is strong and monolithic. It is also seen from Fig. 2 and Fig. 3 that the microstructure of the BPT/GO sample is not free from pores. The cracked sample has numerous pores.

An example of the results of EDS analysis of the BPT/GO composite obtained by us is presented in Fig. 4 (in one selected place of the sample).

The EDS investigations of the BPT/GO composite have also been done in ten other locations, and then averaged and compared with the results of the calculations for the assumed composition (Table 1).

Table 1
Results of EDS investigations of the BPT/GO composite obtained in the ten locations and next averaged and compared with calculations for the assumed composition

Symbol of element	Experimental mol % - averaged from 10 locations	Assumed mol %
C	6.11	1.99
O	-------	
Ti	48.00	49.00
Ba	32.75	28.35
Pb	13.15	19.65

It is seen from Table 1 that a large excess of carbon in experimental results occurs. Probably, it can be related with the fact that the graphite matrix has been used during SPS process. On the other hand, too small lead content and too big barium content can be probably the result evaporation of lead from the sample during sintering. The previously described theoretical value of apparent density at a level lower than expected can be related with this result as well as with a fairly large porosity.

The results of XRD investigations of the BPT/GO composite are shown in Fig. 5. A comparison with standards led us to a conclusion that the most distinct lines correspond to the maxima of $BaTiO_3$, while additional maxima correspond to $Ba_4Ti_{13}O_{30}$, Pb and PbO_2. In Fig. 6b, the maxima of the BPT/GO composite sample with the maxima of commercial graphene oxide (FL-GOc) sample [6] are compared, and the diffractogram of graphite (GR) is presented. It seems that additional maxima do originate neither from FL-GOc nor from GR.

During the preparation of the samples for testing of electrical properties, they were cut along the thickness and then polished. Consecutively, the sample was "tempered" by heating at a temperature of 800 °C in the air. After this operation, the color of the sample changed from black to light beige. Finally, on both surfaces of the sample, the silver paste electrodes were put. Results of the measurement of main dielectric properties vs. temperature are presented in Fig. 6a and Fig. 6b. For this composition of BPT, the maximum of dielectric permittivity (ε') should be observed at temperature 332 °C. Such maximum is seen only for frequencies higher than 20 kHz (see Fig. 6a). For lower frequencies, this maximum is not seen, probably as a result of high electrical conductivity and high dielectric loss (Fig. 6b).

Results of the measurements of main dielectric properties vs. frequency are presented in Fig. 7a and Fig. 7b. Dependencies of $\varepsilon'(f)$ presented in Fig. 7a are rather typical for normal Deby'e relaxation for samples in which electrical conductivity is important. It is also seen in Fig. 7b, at frequencies below 1 kHz, that the values of $\tan\delta$ are many times higher than at higher frequencies.

In Fig. 8a it is presented the results of the measurement of d.c. electrical conductivity $\ln\sigma_{dc}$ v.s. $1000/T$. It is seen from Fig. 8a that the PTCR effect takes place at temperatures up to about 120 °C. In Fig. 8a it is also presented how activations energies E_{a1} and E_{a2} have been calculated.

A.c. electrical conductivity has been calculated from dielectric measurements using the formula:

$$\sigma_{ac} = \omega \cdot \varepsilon_0 . \varepsilon' \cdot \tan\delta, \quad (1)$$

where ω is angular frequency, ε_0 is vacuum permittivity, ε' is a real part of relative permittivity and $\tan\delta$ is the loss tangent. Results of the calculations of a.c. electrical conductivity compared with σ_{dc} are presented in Fig. 8b.

The results of the a.c. and d.c. conductivity tests presented in Fig. 8 show that at low temperatures σ_{ac} is higher than the σ_{dc} and increases with the increasing frequency of the measuring field. This is a rather common behavior for ferroelectric ceramics to which the solid solution of BPT belongs.

The main electro-physical parameters of the obtained BPT/GO composite samples are presented in Table 2.

Table 2
The electro-physical parameters of the BPT/GO composite samples

ρ (g/cm^3)	$\rho_{theoret}$ (g/cm^3)	ε_r [a,b]	$\tan\delta$ [a,b]	T_m [b] (°C)	ε_m at T_m [b]	$\tan\delta$ at T_m [b]	E_{a1} (eV)	E_{a2} (eV)
6.07	6.55	293	0.051	386	1026	1.523	1.81	0.967
[a] - at room temperature, [b] - at 1 kHz								

Results of the investigations of *P-E* hysteresis loops are presented in Fig. 9.

Hysteresis loops below 90 °C are wide and typical for materials with rather high electrical conductivity. In general, these investigations confirm the fact that from room temperature to about 120 °C, electrical conductivity decreases (PTC effect) and, as a result, the hysteresis loops become more typical for ferroelectrics. The obtained values of polarization are rather typical for such a type of ferroelectric materials. Investigations at higher temperatures cannot be possible probably as a result of increasing electrical conductivity with increasing temperature.

4. Conclusions

We describe the technology of obtaining and main physical properties of $Ba_{0.6}Pb_{0.4}TiO_3$/graphene oxide (BPT/GO) ceramic composite with 1.6 wt.% of graphene oxide flakes added. In the final step, the samples have been sintered using the Spark Plasma Sintering (SPS) method. The analysis of SEM microphotograps of the obtained samples shows that the grains are very small and not fully formed. Grains do not have optimal shapes and their breakthrough occurs mainly by seed. However, during cracking the grains do not disintegrate into small fragments i.e. their surface is strong and monolithic. From the investigations of chemical composition using EDS method, we stated that it differs a little from the established one. Diffraction patterns of BPT/GO composite exhibit lines which can be related with perovskite structure, as well as additional lines that can be derived from the initial component oxides. However, there are no visible lines either of graphene oxide (GO) or graphite (GR).

The obtained material, up to about 250 °C, has in general good dielectric properties and low dielectric loss, however the dependencies $\varepsilon'(T)$ and $\tan\delta(T)$ are rather complicated. The dependency $\ln\sigma_{dc}(1000/T)$ suggests that PTCR effect takes place at temperatures up to about 120 °C. For potential applications in microelectronics, PTCR can be interesting. A similar effect has been found, for instance, in ceramics of solid solutions $(Pb_{0.65}Ba_{0.35})TiO_3$ and $(Pb_{0.8}Ba_{0.2})TiO_3$ [4]. Ferroelectric hysteresis loops below 90 °C are wide and typical for materials with rather high electrical conductivity. The hysteresis loop obtained at 120 °C is more typical for ferroelectric material. It can probably be related with the decrease of electrical conductivity with increasing temperature above 120–150 °C. Therefore, we can state that the obtained material is interesting, however it is probably possible to find better conditions of obtaining it and/or a better composition.

References

1. Cai W, Fu C et al (2011) Vanadium doping effects on microstructure and dielectric properties of barium titanate ceramics. Ceram Int 37:3643–3650
2. Pecharromán C, Esteban-Betegón F et al (2001) New percolative $BaTiO_3$-Ni composites with a high and frequency-independent dielectric constant ($\varepsilon_r \approx 80000$). Adv Mater 13:1541–1544
3. Nomura S, Sawada S (1951) Dielectric and thermal properties of barium-lead titanates. J Phys Soc Jpn 6:36–39
4. Wodecka-Duś B, Adamczyk-Habrajska M et al (2018) Electric and dielectric properties of $(Ba_{0.6}Pb_{0.4})TiO_3$ ceramics modified with special glass in the range of phase transition. Processing Application of Ceramics 12:129–135
5. Geim AK (2009) Graphene: Status and Prospects. Science 324:1530–1534
6. Fernández-García L, Suárez M et al (2015) Dielectric behavior of ceramic–graphene composites around the percolation threshold. Nanoscale Res Lett 10:216–223

7. Luo B, Wang X et al (2016) Dielectric Enhancement in Graphene/Barium Titanate Nanocomposites. ACS Appl Mater Interfaces 8:3340–3348
8. Jandhyala S, Mordi G et al (2013) Graphene-ferroelectric hybrid devices for multi-valued memory system. Appl Phys Lett 103:022903–022903
9. Bochenek D, Niemiec P et al (2015) Ferroelectric and magnetic properties of the PMN-PT-nickel zinc ferrite multiferroic ceramic composite materials. Mater Chem Phys 157:116–123
10. Bochenek D, Niemiec P et al (2016) Technology and dielectric properties of the PLZT-NZF composites. Integrated Ferroelectrics 173:82–88
11. Bochenek D, Niemiec P et al (2017) The Basic Properties of the Ferroelectromagnetic Composites Based on Ferrite and PZT-Type Powders. Advances in Science Technology 98:9–14. doi:10.4028/www.scientific.net/AST.98.9
12. Stobinski L, Lesiak B et al (2014) Graphene oxide and reduced graphene oxide studied by the XRD, TEM and electron spectroscopy methods. Journal of Electron Spectroscopy Related Phenomena 195:145–154
13. Stobinski L, Nanomaterials, Warsaw, Poland, Available online: www.nanomaterials.pl; analysis for flake graphene samples: TGA for GO and rGO

Figures

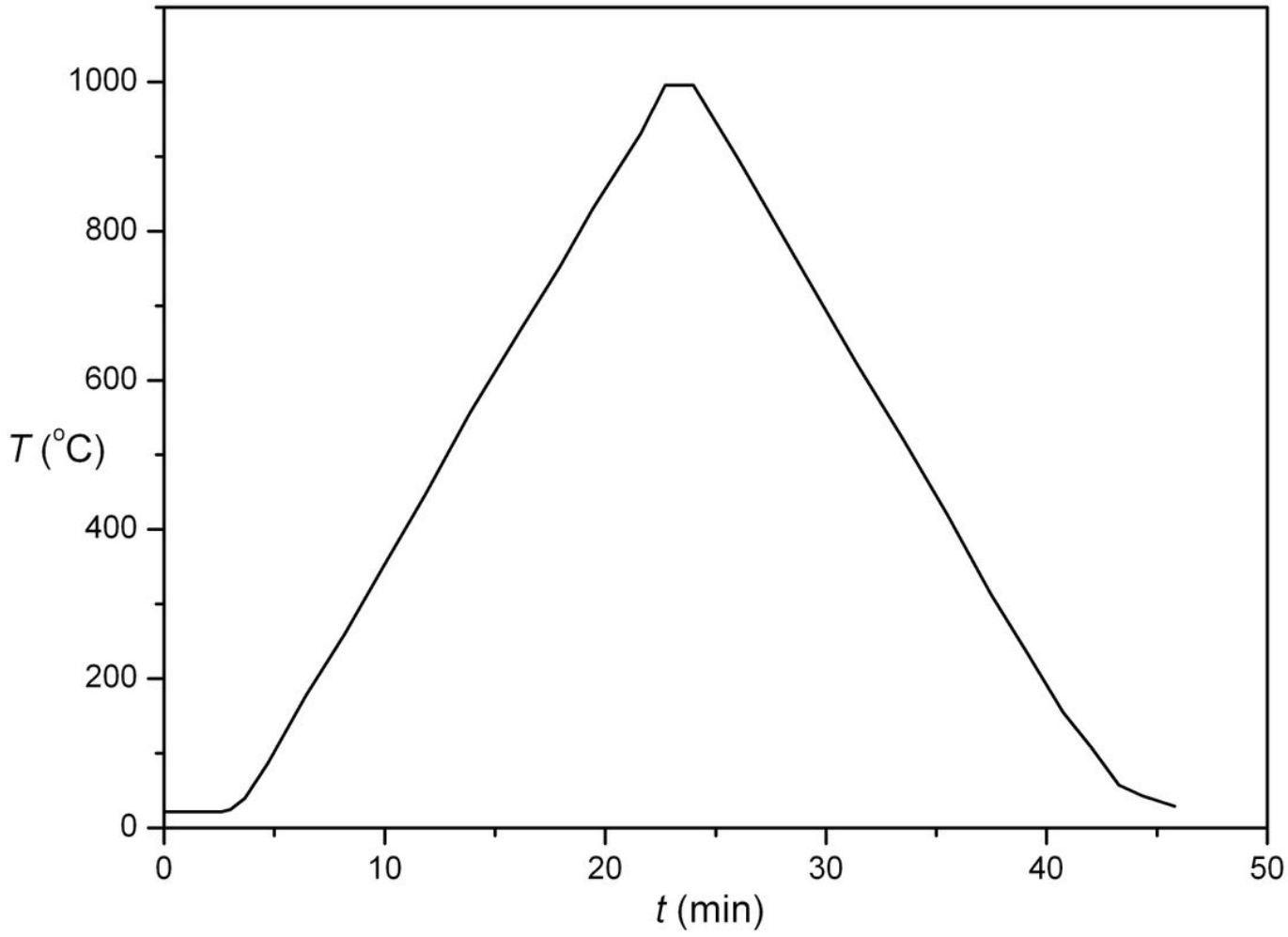

Figure 1

The dependency of temperature vs. time during SPS process. Temperature at maximum was equal to 1000°C. atmosphere argon, pressure 40 MPa

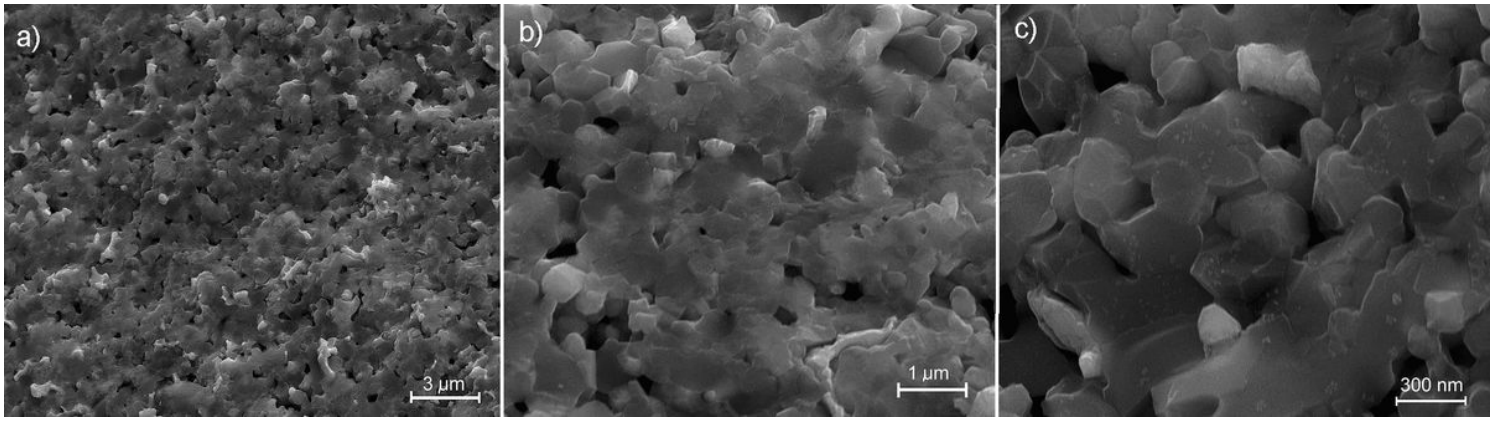

Figure 2

FE-SEM images of obtained by us composite BPT/GO with 1.6 wt.% of GO: magnification a) 5x, b) 15x, c) 30x

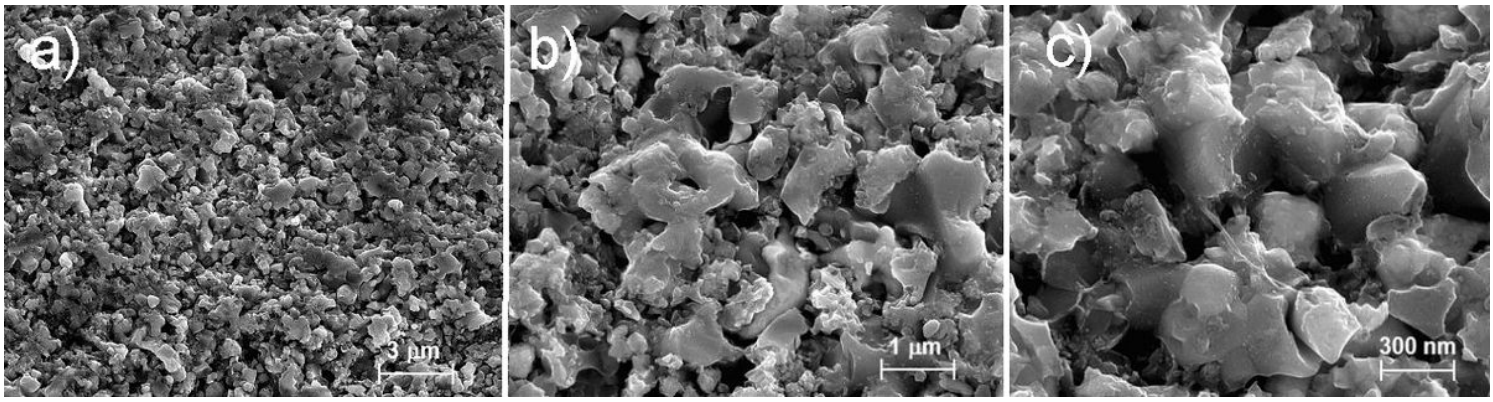

Figure 3

FE-SEM images of the composite BPT/GO with 1.6 wt.% of GO after etching the surface: magnification a) 5x, b) 15x, c) 30x

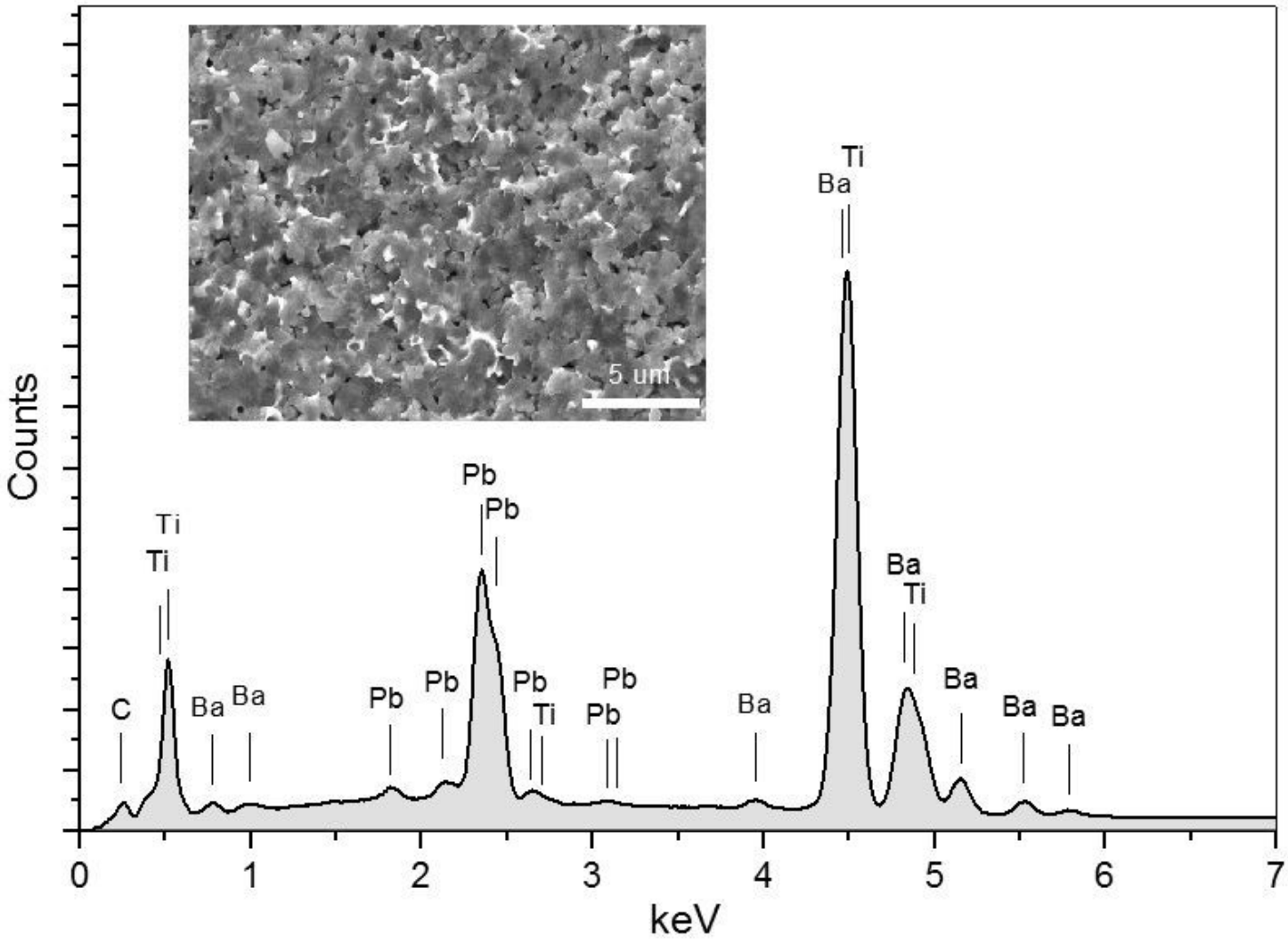

Figure 4

The example of EDS spectrum of BPT/GO composite (with 1.6 wt.% of GO)

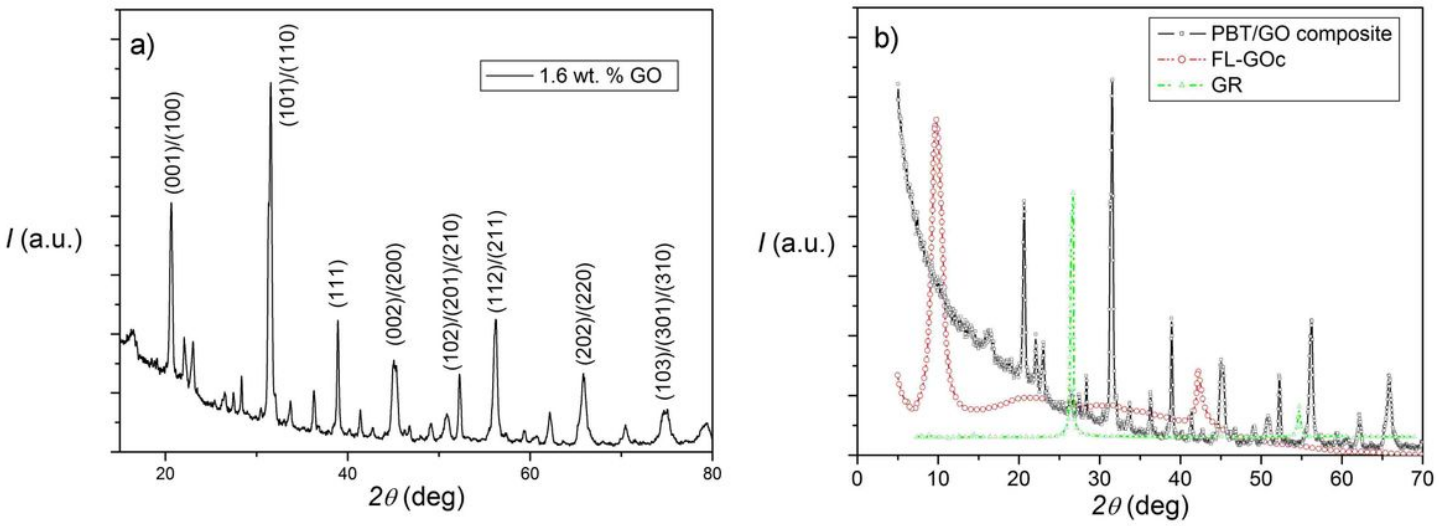

Figure 5

a) XRD pattern of composite sample with 1.6 wt.% of GO. Indexing of maxima is based on comparison with BaTiO3 b) comparison of maxima from Fig. 5a with the maxima of commercial graphene oxide (FL-GOc) - red line and graphite GR - green line - using data from [6]

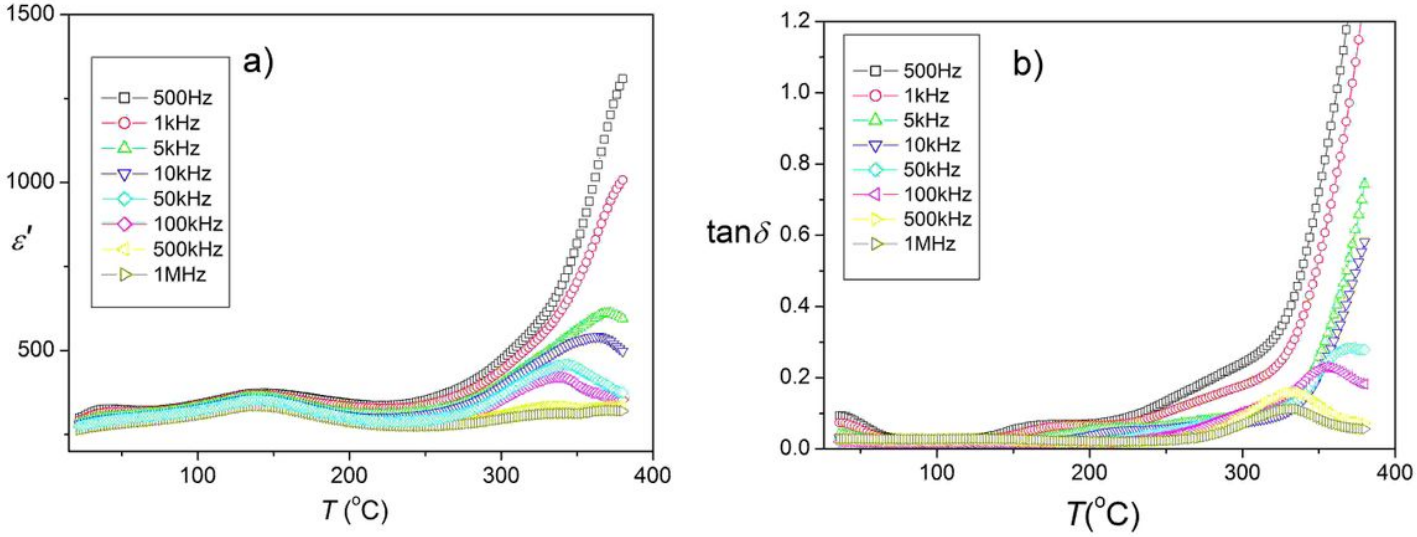

Figure 6

Dependencies ε'(T) (a) and tanδ(T) (b) for BPT/GO composite sample with 1.6 wt.% of GO

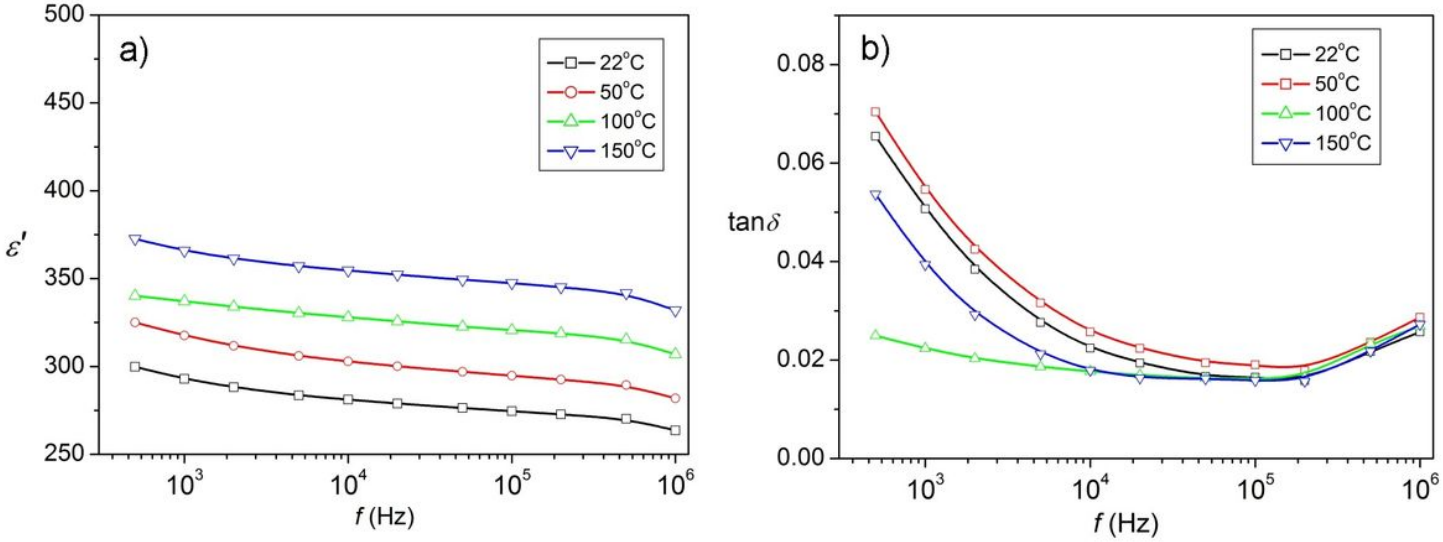

Figure 7

Dependencies ε'(f) (a) and tanδ(f) (b) for BPT/GO composite sample with 1.6 wt.% of GO at various temperatures

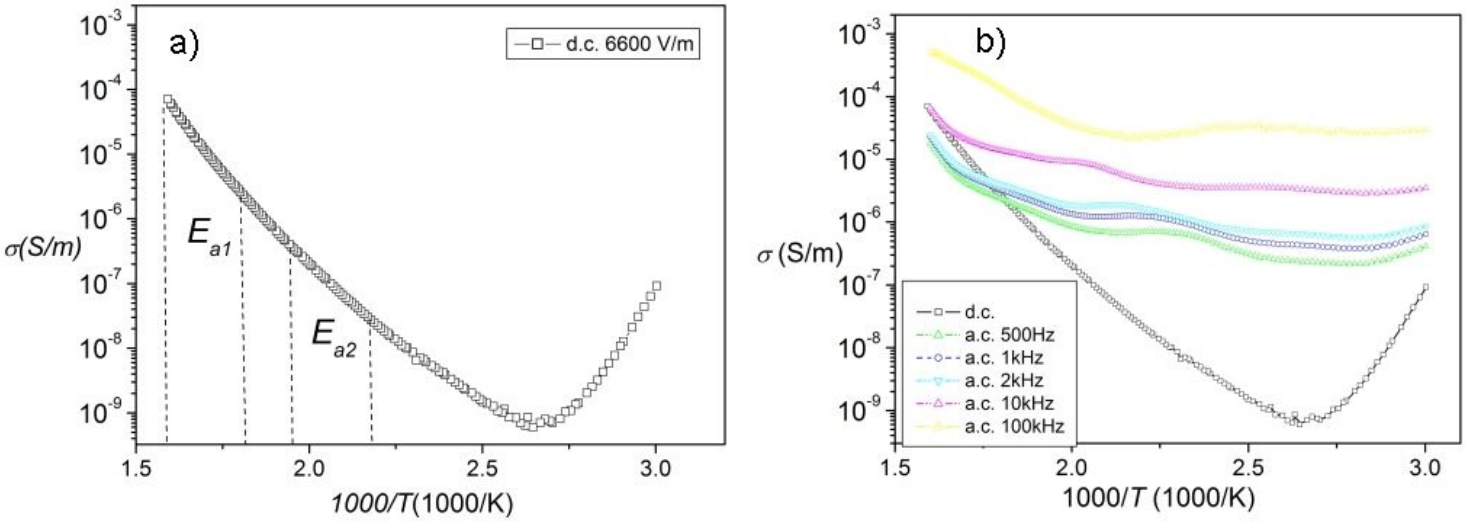

Figure 8

a) the result of the measurement of d.c. electrical conductivity ln□dc v.s. 1000/T and explanation activations energies Ea1 and Ea2 have been calculated b) dependencies □dc(1000/T) at constant measuring field 6600 V/m for BPT/GO composite sample compared with dependencies □ac(1000/T)

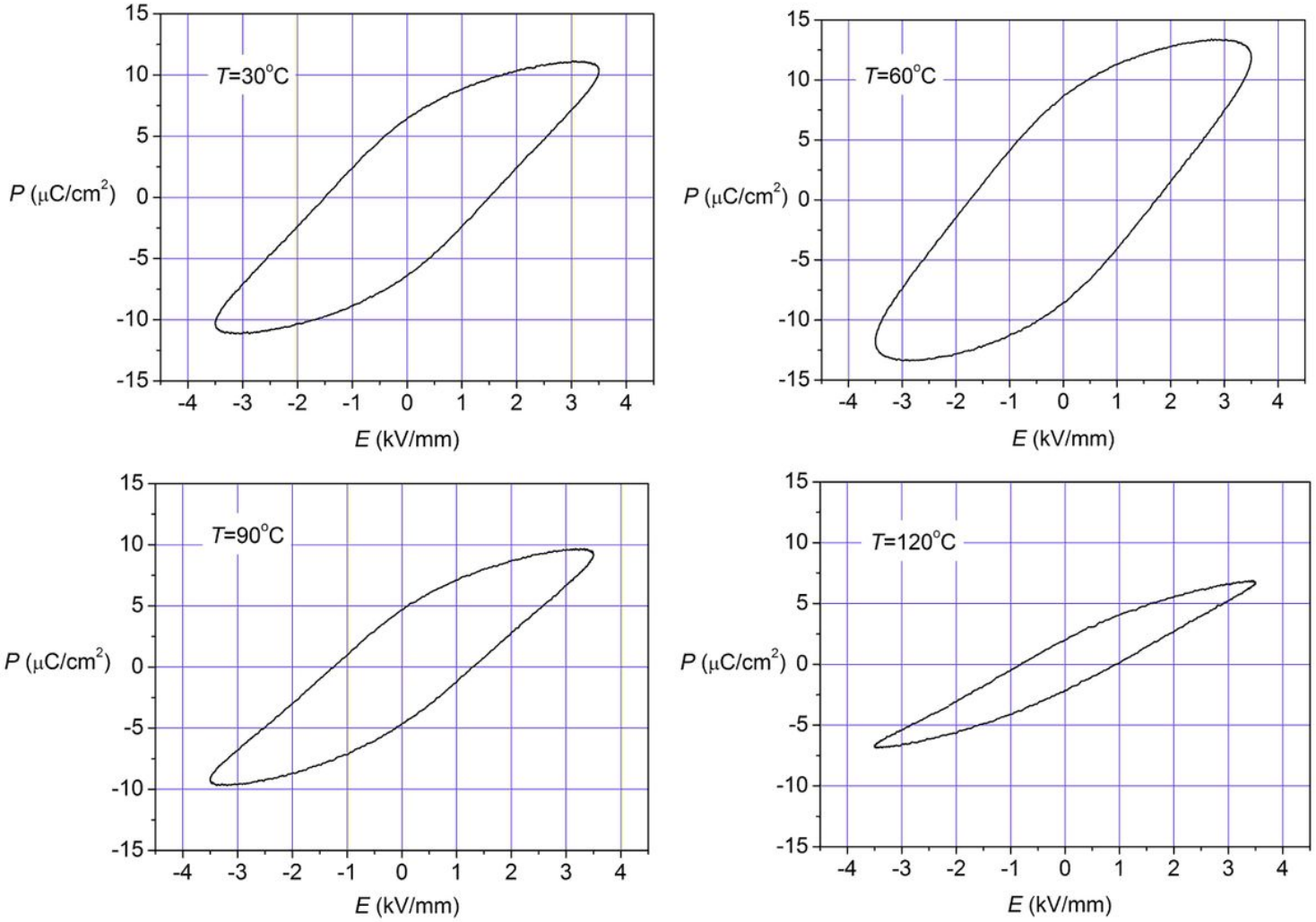

Figure 9

P-E hysteresis loops measured for BPT/GO composite sample with 1.6 wt.% of GO at frequency 1 Hz

Supplementary Files

This is a list of supplementary files associated with this preprint. Click to download.

- supplement15.doc